

# 3D MHD simulations of subsurface convection in OB stars

Matteo Cantiello<sup>1</sup>, Jonathan Braithwaite<sup>1</sup>, Axel Brandenburg<sup>2,3</sup>,  
Fabio Del Sordo<sup>2,3</sup>, Petri Käpylä<sup>2,4</sup>, Norbert Langer<sup>1</sup>

<sup>1</sup>Argelander-Institut für Astronomie der Universität Bonn, Auf dem Hügel 71, D-53121 Bonn, Germany email: [cantiello@astro.uni-bonn.de](mailto:cantiello@astro.uni-bonn.de) <sup>2</sup>NORDITA, AlbaNova University Center, Roslagstullsbacken 23, SE-10691 Stockholm, Sweden <sup>3</sup>Department of Astronomy, AlbaNova University Center, Stockholm University, SE-10691 Stockholm, Sweden <sup>4</sup>Department of Physics, Gustaf Hällströmin katu 2a (PO Box 64), FI-00014, University of Helsinki, Finland

**Abstract.** During their main sequence evolution, massive stars can develop convective regions very close to their surface. These regions are caused by an opacity peak associated with iron ionization. Cantiello et al. (2009) found a possible connection between the presence of sub-photospheric convective motions and small scale stochastic velocities in the photosphere of early-type stars. This supports a physical mechanism where microturbulence is caused by waves that are triggered by subsurface convection zones. They further suggest that clumping in the inner parts of the winds of OB stars could be related to subsurface convection, and that the convective layers may also be responsible for stochastic excitation of non-radial pulsations. Furthermore, magnetic fields produced in the iron convection zone could appear at the surface of such massive stars. Therefore subsurface convection could be responsible for the occurrence of observable phenomena such as line profile variability and discrete absorption components. These phenomena have been observed for decades, but still evade a clear theoretical explanation. Here we present preliminary results from 3D MHD simulations of such subsurface convection.

**Keywords.** convection, hydrodynamics, waves, stars: activity, stars: atmospheres, stars: evolution, stars: magnetic fields, stars: spots, stars: winds, outflows

---

## 1. Introduction

Hot luminous stars show a variety of phenomena in their photospheres and in their winds which still lack a clear physical interpretations at this time. Among these phenomena are photospheric turbulence, line profile variability (LPVs), discrete absorption components (DACs), wind clumping, variable or constant non-thermal X-ray and radio emission, chemical composition anomalies, and intrinsic slow rotation. Cantiello et al. (2009) argued that a convection zone close to the surface of hot, massive stars, could be responsible for various of these phenomena. This convective zone is caused by a peak in the opacity due to iron recombination and for this reason is referred as the “iron convection zone” (FeCZ). A physical connection may exist between microturbulence in hot star atmospheres and a subsurface FeCZ. The strength of the FeCZ is predicted to increase with increasing metallicity  $Z$ , decreasing effective temperature  $T$  and increasing luminosity  $L$ , and all three predicted trends are reflected in observational data of microturbulence obtained in the context of the VLT-FLAMES survey of massive stars (Evans et al. 2005). Moreover recent measurements of microturbulence (Fraser et al. 2010) are in agreement with the results of Cantiello et al. (2009). This suggests that microturbulence corresponds to a physical motion of the gas in hot star atmospheres. This motion may then be connected to wind clumping, since the empirical microturbulent velocities are comparable to the local sound speed at the stellar surface.

The FeCZ in hot stars might also produce localized surface magnetic fields (Cantiello et al. 2009). Such magnetic fields may become buoyant and reach the surface, creating magnetic spots. This could explain the occurrence of DACs (discrete absorption components in UV absorption lines), also in very hot main sequence stars for which pulsational instabilities are not predicted. Moreover there may be regions of the upper HR diagram for which the presence of the FeCZ influences, or even excites, non-radial stellar pulsations. Interestingly stochastic excitation of non-radial pulsations has been recently found in massive stars (Belkacem et al. 2009; Degroote et al. 2010).

The FeCZ could also turn out to directly affect the evolution of hot massive stars. If it induces wind clumping, it may alter the stellar wind mass-loss rate. Such a change would also influence the angular momentum loss. In addition, magnetic fields produced by the iron convection zone could lead to an enhanced rate of angular momentum loss. These effects become weaker for lower metallicity, where the FeCZ is less prominent or absent.

Finally, the consequences of the FeCZ might be strongest in Wolf-Rayet stars. These stars are so hot that the iron opacity peak, and therefore the FeCZ, can be directly at the stellar surface, or — to be more precise — at the sonic point of the wind flow (Heger & Langer 1996). This may relate to the very strong clumping found observationally in Wolf-Rayet winds (Lépine & Moffat 1999; Marchenko et al. 2006), and may be required for an understanding of the very high mass-loss rates of Wolf-Rayet stars (Eichler et al. 1995; Kato & Iben 1992; Heger & Langer 1996).

## 2. Simulations of subsurface convection

Convection in the FeCZ is relatively inefficient: the transport of energy is dominated by radiation, which usually accounts for more than 95% of the total flux. This region of the star is very close to the photosphere, above which strong winds are accelerated. The continuous loss of mass from the stellar surface moves the convection region to deeper layers, revealing to surface material that has been processed in the FeCZ. In rotating stars, the associated angular momentum loss might also drive strong differential rotation in the region of interest. It is clear that, under these circumstances, the mixing length theory can only give a qualitative picture of the convective properties in these layers. In order to study the effects induced by the presence of subsurface convection at the stellar surface in a more quantitative way, we perform local 3D MHD calculations of convection. In these simulations we can vary the relative importance of the background radiative flux and include the effects of rotation and shear, in order to model conditions as similar as computationally permitted to subsurface convection in OB stars.

### 2.1. Computational model

The setup is similar to that used by Käpylä et al. (2008). A rectangular portion of a star is modeled by a box situated at colatitude  $\theta$ . The dimensions of the computational domain are  $(L_x, L_y, L_z) = (5, 5, 5)d$  where  $d$  is the depth of the convectively unstable layer. Our  $(x, y, z)$  correspond to  $(\theta, \phi, r)$  in spherical polar coordinates. The box is divided into three layers, an upper cooling layer, a convectively unstable layer, and a stable overshoot layer (see below). The following set of equations for compressible magnetohydrodynamics is being solved:

$$\frac{\partial \mathbf{A}}{\partial t} + Sx \frac{\partial \mathbf{A}}{\partial y} = \mathbf{U} \times \mathbf{B} - \eta \mu_0 \mathbf{J} - SA_y \hat{\mathbf{x}}, \quad (2.1)$$

$$\frac{D \ln \rho}{Dt} = -\nabla \cdot \mathbf{U}, \quad (2.2)$$

$$\frac{D\mathbf{U}}{Dt} = -\frac{1}{\rho}\nabla p + \mathbf{g} - 2\boldsymbol{\Omega} \times \mathbf{U} + \frac{1}{\rho}\mathbf{J} \times \mathbf{B} + \frac{1}{\rho}\nabla \cdot 2\nu\rho\mathbf{S} - S\mathbf{U}_x\hat{\mathbf{y}}, \quad (2.3)$$

$$\frac{De}{Dt} = -\frac{p}{\rho}\nabla \cdot \mathbf{U} + \frac{1}{\rho}\nabla \cdot K\nabla T + 2\nu\mathbf{S}^2 + \frac{\eta}{\rho}\mu_0\mathbf{J}^2 - \frac{e-e_0}{\tau(z)}, \quad (2.4)$$

where  $D/Dt = \partial/\partial t + (\mathbf{U} + \bar{\mathbf{U}}_0) \cdot \nabla$ , and  $\bar{\mathbf{U}}_0 = (0, Sx, 0)$  is an imposed large-scale shear flow in the  $y$ -direction. The magnetic field is written in terms of the magnetic vector potential,  $\mathbf{A}$ , with  $\mathbf{B} = \nabla \times \mathbf{A}$ ,  $\mathbf{J} = \mu_0^{-1}\nabla \times \mathbf{B}$  is the current density,  $\mu_0$  is the vacuum permeability,  $\eta$  and  $\nu$  are the magnetic diffusivity and kinematic viscosity, respectively,  $K$  is the heat conductivity,  $\rho$  is the density,  $\mathbf{U}$  is the velocity,  $\mathbf{g} = -g\hat{\mathbf{z}}$  is the gravitational acceleration, and  $\boldsymbol{\Omega} = \Omega_0(-\sin\theta, 0, \cos\theta)$  is the rotation vector. The fluid obeys an ideal gas law  $p = (\gamma - 1)\rho e$ , where  $p$  and  $e$  are pressure and internal energy, respectively, and  $\gamma = c_p/c_v = 5/3$  is the ratio of specific heats at constant pressure and volume, respectively. The specific internal energy per unit mass is related to the temperature via

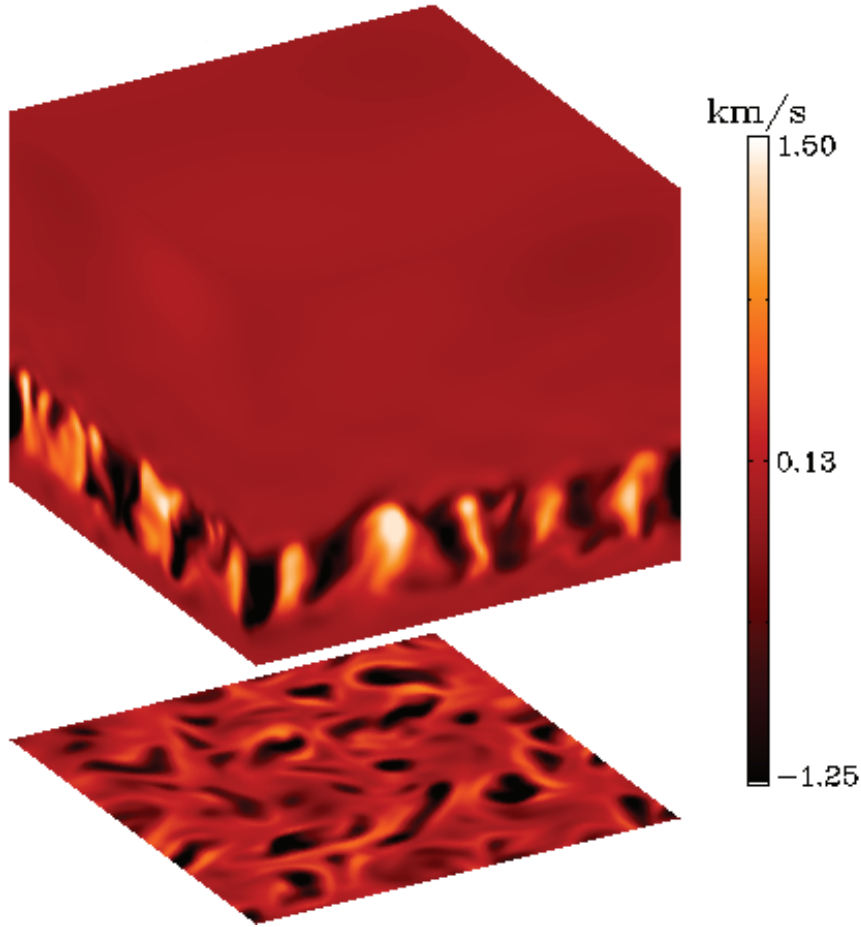


**Figure 1.** Simulation of subsurface convection. Starting from the top, the box is divided into three layers: a radiative layer with an upper cooling boundary, a convectively unstable layer and another stable layer at the bottom. The snapshot shows values of vertical velocity. The plane below the box shows the vertical velocity field at the lower boundary of the convective layer.

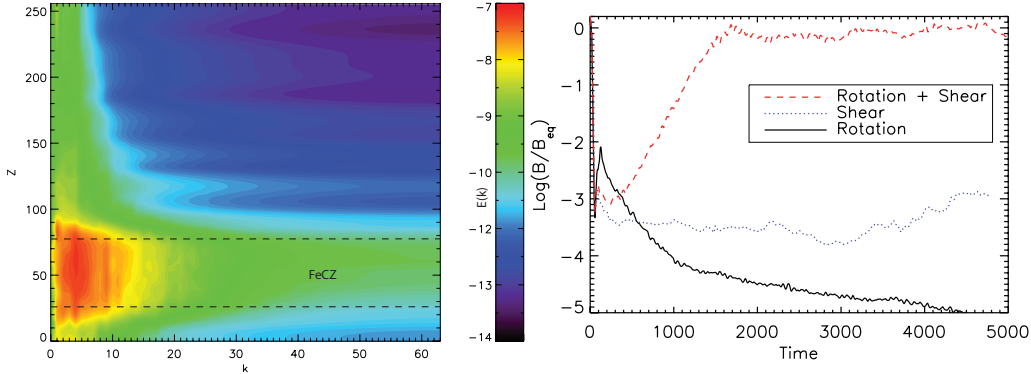


**Figure 2.** **Left:** evolution of the magnetic field as function of time (in code units) in three different runs with different physics. The value on the  $y$ -axis is the logarithm of the ratio between the magnetic field and the equipartition value (the value corresponding to equipartition between kinetic and magnetic energy). Dynamo action reaching equipartition is found in simulations including both rotation and shear. **Right:** energy spectrum of the velocity field in our run of subsurface convection. On the  $x$ -axis is the spatial wavenumber  $k$ , on the  $y$ -axis the  $z$  coordinate of the computational domain in gridpoints. The color bar on the right indicates the value of the energy per wavenumber  $E(k)$ . The location of the convection zone in the  $z$ -coordinate is shown by the dashed lines, the rest of the domain is radiative. Just above and below the convection zone kinetic energy is associated with overshooting, while at further distances the transport of energy is facilitated by gravity waves.

$e = c_V T$ . The rate of strain tensor  $\mathbf{S}$  is given by

$$S_{ij} = \frac{1}{2}(U_{i,j} + U_{j,i}) - \frac{1}{3}\delta_{ij}\nabla \cdot \mathbf{U}. \quad (2.5)$$

The last term of Eq. (2.4) describes cooling at the top of the domain. Here  $\tau(z)$  is a cooling time which has a profile smoothly connecting the upper cooling layer and the convectively unstable layer below, where  $\tau \rightarrow \infty$ .

The positions of the bottom of the box, bottom and top of the convectively unstable layer, and the top of the box, respectively, are given by  $(z_1, z_2, z_3, z_4) = (-0.5, 0, 1, 4.5)d$ , where  $d$  is the depth of the convectively unstable layer. Initially the stratification is piecewise polytropic with polytropic indices  $(m_1, m_2, m_3) = (3, 0.9, 3)$ , which leads to a convectively unstable layer between two stable layers. The cooling term leads to a stably stratified isothermal layer at the top. All simulations with rotation use  $\theta = 0^\circ$  corresponding to the north pole.

Stress-free boundary conditions are used in the vertical ( $z$ ) direction for the velocity,

$$U_{x,z} = U_{y,z} = U_z = 0, \quad (2.6)$$

where commas denote partial derivatives, and perfect conductor conditions are used for the magnetic field, i.e.

$$B_{x,z} = B_{y,z} = B_z = 0. \quad (2.7)$$

In the  $x$  and  $y$  directions periodic boundary conditions are used. The simulations were performed with the PENCIL CODE<sup>†</sup>, which uses sixth order explicit finite differences in space and third order accurate time stepping method. Resolutions of up to  $128^2 \times 256$  mesh points were used.

<sup>†</sup> <http://pencil-code.googlecode.com/>

### 2.2. Preliminary results

As a preliminary study we performed low resolution simulations (128x128x256), where the density contrast between the bottom of the convective layer and the top of the domain is only  $\sim 20$ . This is about ten times smaller than in the case of the FeCZ. Moreover the ratio of the convective to radiative flux is about 0.3, higher than in the FeCZ case. This is because smaller values of convective flux result in steady convection at the low resolution of these preliminary runs. Therefore, at this stage, the velocities of convective motions cannot directly be compared to the velocities obtained by mixing length theory. However already in these preliminary runs we could follow the excitation and propagation of gravity waves above the convective region. In the right panel of Fig. 2 we show the kinetic energy spectrum (as function of the spatial wavenumber  $k$ ) in the horizontal plane, as function of depth. The maximum of energy is found in the convective region for those wavenumbers  $k$  corresponding to the number of resolved convective cells (about 5 along one of the horizontal directions). Energy is also transported up to the top layer by gravity waves, where the maximum of the energy is deposited in those wavelengths that are resonant with the scale of convective motions, as predicted, for example, by Goldreich & Kumar (1990).

Käpylä et al. (2008) found excitation of a large scale dynamo in simulations of turbulent convection including rotation and shear. Our computational setup is very similar, so it's not surprising that we can confirm this result. Dynamo action reaching equipartition is found in our simulations that include shear and rotation (see left panel of Fig. 2), with magnetic fields on scales larger than the scale of convection.

### 2.3. Discussion

The connection found by Cantiello et al. (2009) between the presence of sub-photospheric convective motions and microturbulence in early-type stars is intriguing. The recent identification of solar-like oscillations in hot massive stars (Belkacem et al. 2009; Degroote et al. 2010) and further measurements of microturbulence (Fraser et al. 2010) also point toward a picture in which the FeCZ influences surface properties of OB stars.

We performed 3D MHD simulations of convection to investigate the excitation and propagation of gravity waves above a subsurface convection zone. Analytical predictions of Goldreich & Kumar (1990) on the spatial scale at which the maximum of energy is injected in gravity waves seem to be confirmed in our preliminary calculations. Further investigation is required to understand if the subsurface convection expected in OB stars excites gravity waves of the required amplitude to explain the observed microturbulence in massive stars. In particular we need higher resolution to increase the Reynolds number of our simulations and be able to decrease the ratio of convective to radiative flux, which appear to be an important parameter in determining the convective velocities (Brandenburg et al. 2005).

Magnetic fields reaching equipartition values are found in simulations of turbulent convection if rotation and shear are present (Käpylä et al. 2008). Since massive stars are usually fast rotators, it could be that the interplay between convection, rotation and shear is able to drive a dynamo in OB stars. Indeed our simulations of subsurface convection including rotation and shear show the excitation of dynamo action, with magnetic fields reaching equipartition. This means that fields up to a kG could be present in the FeCZ. These magnetic fields might experience buoyant rise and reach the surface of OB stars, where they could have important observational consequences. In particular it has already been suggested that the discrete absorption components observed in UV lines of massive stars could be produced by low amplitude, small scale magnetic fields at the stellar surface (Kaper & Henrichs 1994). Further study is needed to investigate the amplitude

and geometry of magnetic fields reaching the stellar surface, as well as their effects on the photosphere.

## References

- Belkacem, K., Samadi, R., Goupil, M., et al. 2009, *Science*, 324, 1540
- Brandenburg, A., Chan, K. L., Nordlund, Å., & Stein, R. F. 2005, *Astron. Nachr.*, 326, 681
- Cantiello, M., Langer, N., Brott, I., et al. 2009, *Astron. Astrophys.*, 499, 279
- Degroote, P., Briquet, M., Auvergne, M., et al. 2010, *Astron. Astrophys.*, 519, A38
- Eichler, D., Bar Shalom, A., & Oreg, J. 1995, *Astrophys. J.*, 448, 858
- Evans, C., Smartt, S., Lennon, D., et al. 2005, *The Messenger*, 122, 36
- Fraser, M., Dufton, P. L., Hunter, I., & Ryans, R. S. I. 2010, *Mon. Not. Roy. Astron. Soc.*, 404, 1306
- Goldreich, P. & Kumar, P. 1990, *Astrophys. J.*, 363, 694
- Heger, A. & Langer, N. 1996, *Astron. Astrophys.*, 315, 421
- Kaper, L. & Henrichs, H. F. 1994, *Astrophys. Space Sci.*, 221, 115
- Käpylä, P. J., Korpi, M. J., & Brandenburg, A. 2008, *Astron. Astrophys.*, 491, 353
- Kato, M. & Iben, I. J. 1992, *Astrophys. J.*, 394, 305
- Lépine, S. & Moffat, A. F. J. 1999, *Astrophys. J.*, 514, 909
- Marchenko, S. V., Moffat, A. F. J., St-Louis, N., & Fullerton, A. W. 2006, *Astrophys. J.*, 639, L75